Nuclear Forces and Nuclear Energetics*

LESTER INGBER*†‡ AND ROBERT M. POTENZA
Institute for Pure and Applied Physical Sciences, University of California at San Diego, La Jolla, California 92037
(Received 22 May 1969)

Both a static and a momentum-dependent potential are derived from one-meson-exchange Born amplitudes, and are adjusted to fit (i) the deuteron binding energy and quadrupole moment, (ii) S, P, and D partial waves from 25 to 310 MeV, and (iii) the binding energy and saturation property of nuclear matter. This is possible through a different form of the central and tensor potentials which has not been used previously to calculate problems (i), (ii), and (iii) above. We find the σ meson unsuitable to describe the two-pion-exchange region in that a potential with meson parameters common to all partial waves is not achieved.

I. INTRODUCTION

A. Purpose

THE main purpose of this paper is to present a nucleon-nucleon potential which describes properties of (i) the deuteron (binding energy and quadrupole moment), (ii) nucleon-nucleon scattering (represented by data at 25-, 50-, 95-, 150-, 210-, and 310-MeV incident laboratory energy[1]), and (iii) nuclear matter, as described by Brueckner and Masterson[2] (binding energy and saturation property at internucleon separations appropriate to infinite nuclear matter). We show why these three problems are suitable to test the shape of this potential in the nonrelativistic region [here defined for $r>\hbar(mc)^{-1}$, where $mc^2=0.938$ BeV]. We present detailed calculations giving a new functional form of the coupled ${}^3S_1$-${}^3D_1$ partial-wave potentials which enables us to achieve agreement with the experimental data of problems (i), (ii), and (iii) above. This is done by using a momentum-dependent potential derived from a nonrelativistic reduction of one-boson-exchange Feynman amplitudes for nucleon-nucleon scattering. We show that only the gross structure of the momentum dependence need be included to obtain this agreement by obtaining similar results with a static potential. We further show why we are unable to obtain a nucleon-nucleon potential which would be defined as a Born amplitude before a partial-wave reduction is made. That is, our potential is really a set of potentials, each defined in a given partial wave. We present calculations which strongly suggest this is because the physics of the two-pion-exchange region $[\hbar(\mu c)^{-1}>r>\hbar(2\mu c)^{-1}$, where $\mu c^2=0.135$ BeV] has not yet been established.

B. Background

In this paper, we are concerned with obtaining an on-energy-shell nonrelativistic potential to be used in Schrödinger and in Lippmann-Schwinger equations. This potential contains as much meson-baryon physics in the form of one-boson exchanges as we are capable of introducing into detailed calculations of the three problems (i), (ii), and (iii) above. Important progress has been made by Blankenbecler and Sugar,[3] who have emphasized a covariant method of reducing four-dimensional relativistic scalar potentials and Green's functions, as used to solve Bethe-Salpeter-type equations, to their nonrelativistic three-dimensional counterparts, as used to solve Lippmann-Schwinger-type equations. Their most important contribution pertinent to this work is to give a formalism capable of including higher-order relativistic corrections arising from nucleon negative-energy states, and from kinematic momentum-dependence factors of the nonrelativistic scattering amplitude.

Because the mathematical structure of these one-boson-exchange potentials is rather simple, we feel it is worthwhile to use such interactions in the coordinate r-space Schrödinger representation. One confusion that can arise concerns the difference between energy and momentum dependence. In both the Born approximation and in the asymptotic, large-r region in the coordinate space representation, the two are of course equivalent. This was noted by Wong, who suggested that the nucleon-nucleon potential be defined by the second-order Feynman amplitude for nucleon-nucleon scattering.[4] We now emphasize the difference in interpretation of the potential in the coordinate space and in the asymptotic momentum-space scattering formalisms; we also spell out what we mean when we state that problems (i), (ii), and (iii) above are solved *consistently* when using these potentials in coordinate space.

* Research supported by the U.S. Atomic Energy Commission under Contract No. AT(11-1)-GEN-10, P.A. 11: Report No. UCSD-10P11-94 and the National Science Foundation.
† National Science Foundation Postdoctoral Fellow.
‡ Present address: Physics Department, State University of New York at Stony Brook, Stony Brook, N.Y. 11790.
[1] M. H. MacGregor, R. A. Arndt, and A. A. Dubow, Phys. Rev. **135**, B628 (1964); M. H. MacGregor and R. A. Arndt, *ibid.* **139**, B362 (1965); H. P. Noyes, D. S. Bailey, R. A. Arndt, and M. H. MacGregor, *ibid.* **139**, B380 (1965). There is still some uncertainty as to the sign and magnitude of ϵ_1 at 25 MeV; see M. H. MacGregor, R. A. Arndt, and R. M. Wright, *ibid.* **173**, 1272 (1968); R. E. Seamon, K. A. Freidman, G. Breit, R. D. Haracz, J. M. Holt, and A. Prakash, *ibid.* **165**, 1579 (1968).
[2] K. A. Brueckner and K. S. Masterson, Jr., Phys. Rev. **128**, 2267 (1962).
[3] R. Blankenbecler and R. Sugar, Phys. Rev. **142**, 1051 (1966).
[4] D. Y. Wong, Nucl. Phys. **55**, 212 (1964).

For two nucleons of relative momenta $\mathbf{k}$, elastically scattering into states of relative momenta $\mathbf{k}'(k^2 = k'^2)$, the (generally) nonlocal, nonrelativistic potential is defined by

$$V(\mathbf{r}, \mathbf{r}') = (2\pi)^{-3} \int d^3k\, d^3k' \exp(i\mathbf{k}'\cdot\mathbf{r}') M(\mathbf{k}, \mathbf{k}') \times \exp(-i\mathbf{k}\cdot\mathbf{r}), \quad (1.1)$$

where $M(\mathbf{k}, \mathbf{k}')$ is the invariant amplitude multiplied by $m(m^2 + k^2)^{-1/2}$. Application of the unitarity condition to the scattering matrix, or demanding invariance when calculating the differential cross section, dictates that

$$[\text{relativistic transition amplitude}]:[\text{invariant amplitude}]:[\text{nonrelativistic transition (potential) amplitude}] \sim m^{-1}(m^2 + k^2)^{1/2}:1:m(m^2 + k^2)^{-1/2}.$$

These factors give rise to what is popularly called "minimal relativity." There are actually five such independent invariant amplitudes for elastic nucleon-nucleon scattering[4] which can be conveniently transformed into coordinate-space potentials for use in Schrödinger's equation after a partial-wave reduction[5] (see NF-Sec. II and NF-Appendix B). In coordinate space, a convenient set is V_C(central), V_T(tensor) V_{LS}(spin orbit), V_σ(spin spin), and $V_{\sigma p}$(spin momentum).

This potential is unitarized via Schrödinger's equation:

$$(E - k^2/m)\psi_E(\mathbf{r}) = \int d^3r' V(\mathbf{r}, \mathbf{r}')\psi_E(\mathbf{r}'), \quad (1.2)$$

where $k^2 = -\hbar^2\nabla_r^2$ and E is the total nonrelativistic energy of the two nucleons. Writing $E = q^2/m$, Eq. (1.2) may be rewritten

$$(\nabla_r^2 + q^2)\psi_q(\mathbf{r}) = m \int d^3r' V(\mathbf{r}, \mathbf{r}')\psi_q(\mathbf{r}'). \quad (1.3)$$

Denoting the solution to Eq. (1.3) by $\chi_q(\mathbf{r})$ when $V(\mathbf{r}, \mathbf{r}') = 0$, and denoting $G^q(\mathbf{r}, \mathbf{r}')$ as the Green's-function solution to

$$(\nabla_r^2 + q^2)G^q(\mathbf{r}, \mathbf{r}') = \delta(\mathbf{r} - \mathbf{r}'), \quad (1.4)$$

$G^q(\mathbf{r}, \mathbf{r}')$ may be written

$$G_q(\mathbf{r}, \mathbf{r}') = \int d^3q'' \chi_{q''}^*(\mathbf{r}')\chi_{q''}(\mathbf{r})/(q^2 - q''^2). \quad (1.5)$$

The Lippmann-Schwinger integral equation may then be written for $\psi_q(r)$:

$$\psi_q(\mathbf{r}) = \chi_q(\mathbf{r}) + m \int d^3\mathbf{r}' G^q(\mathbf{r}, \mathbf{r}') d^3\mathbf{r}'' V(\mathbf{r}', \mathbf{r}'')\psi_q(\mathbf{r}''). \quad (1.6)$$

Multiplying on the left-hand side of Eq. (1.6) by $\int d^3r''' \chi_{q'}^*(r''') V(\mathbf{r}, \mathbf{r}''')$, simplifying, and comparing the result with the momentum-space equation, one obtains

$$T_{q,q'} = V_{q,q'} + (\text{principal value})m \times \int d^3q'' V_{q,q''} g_{q'',q'} T_{q'',q'}, \quad (1.7)$$

where

$$g_{q'',q'} = (q''^2 - q'^2)^{-1}, \quad (1.8)$$

and one identifies

$$V_{q,q'} = \int d^3r d^3r' \chi_{q'}^*(\mathbf{r}') V(\mathbf{r}, \mathbf{r}')\chi_q(\mathbf{r}), \quad (1.9)$$

where q^2 and q' are now the asymptotic momentum-squared and energy variables of Eq. (1.7); in Eq. (1.1), we defined $V(\mathbf{r}, \mathbf{r}')$ as the Fourier transforms with respect to k and k' which were momentum variables. We consider the following two special cases:

Case 1. If $M(\mathbf{k}, \mathbf{k}') = M_1(\mathbf{k} - \mathbf{k}')$, then $V(\mathbf{r}, \mathbf{r}') = V_1(\mathbf{r}')\delta(\mathbf{r}' - \mathbf{r})$, and a static, local potential is obtained.

Case 2. If $M(\mathbf{k}, \mathbf{k}') = M_2(\mathbf{k} - \mathbf{k}'; k^2 = k'^2)$, where M_2 is expressed as a polynomial in k^2, then $V(\mathbf{r}, \mathbf{r}') = V_2(\mathbf{r}', \nabla_{r'})\delta(\mathbf{r}', -\mathbf{r})$, and a momentum-dependent local potential is obtained.

In a previous paper by one of us,[5] calculations of problems (ii) and (iii) above were done using momentum-dependent potentials as in case 2. To accomplish this, expansions of factors like $m^2(m^2 + k^2)^{-1}$ were carried out to order $k^2(m)^{-2}$. The same basic potentials for the mesons considered in NF-Appendix A (π, σ, η, ρ, ω, and φ) were used here, except for the differences to be stated.

C. Outline

The present work was initiated because of the justifiable criticism that although NF was successful in calculating the correct binding energy of nuclear matter, that work did not attempt to use the deuteron problem, (i) above, to constrain the nucleon-nucleon interaction. In Sec. II, a description of the three physics problems as included in these calculations is given. In Sec. III, the details of these calculations are given, using both the momentum-dependent potential and a static potential with a similar functional form. These results are compared to those obtained using another current popular potential. Here it is shown how the extra binding energy in nuclear matter is achieved as a result of a different ratio of the central-to-tensor potentials than has previously been used. It is shown how this new ratio can be maintained with a static potential, and similar results for the binding energy of nuclear matter are obtained. Examination of the regions of sensitivity of the three problems (i), (ii), and (iii) above shows why the binding energy of nuclear matter is so sensitive to the binding energy of the deuteron. In Sec. IV, the role of the unobserved σ meson at $\sim$400 MeV is found unsuitable to describe the two-pion region for which it was created to simulate. In the conclusion in Sec. V, we summarize the importance of recent calculations in the two-pion region in light of these calculations. Atomic units ($\hbar = c = 1$) will be used throughout this paper, unless explicitly written otherwise.

[5] L. Ingber, Phys. Rev. **174**, 1250 (1968), referred to as NF in this paper.

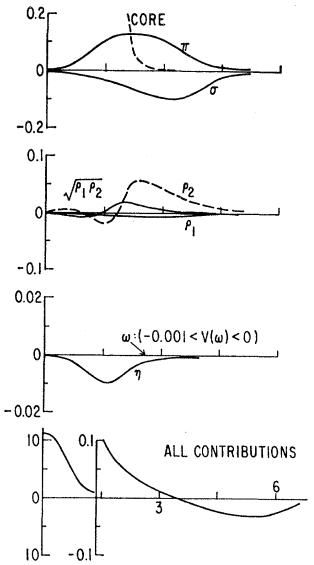

FIG. 1. Contribution of each meson to the static part of the interaction potential (BeV) versus $r(\text{BeV}/\hbar c)^{-1}$ in the ${}^3S_1$ state. Parameters are from the deuteron $+{}^3S_1+{}^3D_1+\epsilon$ "static" fit. The contribution of the mixed tensor part from ρ-meson exchange is indicated by $(P_1\rho_2)^{1/2}$. [See NF-Eq. (2.4) for definitions of g_{ρ_1} and g_{ρ_2}.]

II. DEUTERON, PHASE SHIFTS, AND NUCLEAR-MATTER COMPUTATIONS

A. Problem (i)—Deuteron

As outlined in NF-Sec. V, the coupled ${}^3S_1$- and ${}^3D_1$-state wave functions were calculated by solving matrix equations: the integral equations satisfied by u and w. The S and D state radial components of the deuteron are

$$(\gamma r)^{-1}\begin{pmatrix}u(r)\\ w(r)\end{pmatrix}=\gamma m\int r'^2\,dr' \times\begin{pmatrix} j_0(i\gamma r_<)h_0(i\gamma r_>) & 0\\ 0 & j_2(i\gamma r_<)h_2(i\gamma r_>)\end{pmatrix} \times\begin{pmatrix} V_S(r',d/dr') & V_T(r',d/dr')\\ V_T(r',d/dr') & V_D(r',d/dr')\end{pmatrix}\begin{pmatrix}u(r')\\ w(r')\end{pmatrix}(\gamma r')^{-1}, \tag{2.1}$$

where j_l and h_l are spherical Bessel and Hankel functions of order l, respectively. The quantity $r_<$ ($r_>$) is the lesser (greater) of r and r', $\gamma=(-m\epsilon)^{1/2}$, $m=0.938$ BeV/c^2, $\epsilon=-2.22452$ MeV. The function V_S is the S-state potential as published in NF, and similarly,

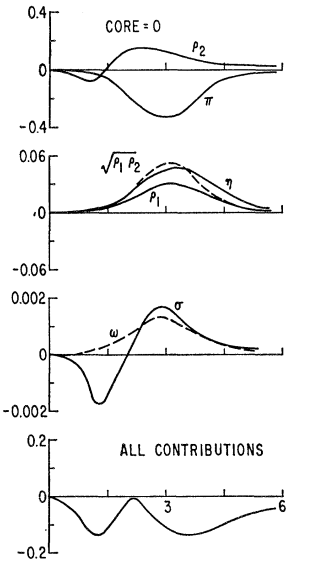

FIG. 2. Contribution of each meson to the static part of the interaction potential (BeV) versus $r(\text{BeV}/\hbar c)^{-1}$ for the tensor part of the ${}^3S_1$-${}^3D_1$ system.

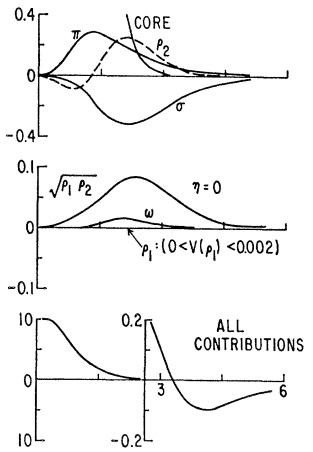

FIG. 3. Contribution of each meson to the static part of the interaction potential (BeV) versus $r(\text{BeV}/\hbar c)^{-1}$ in the ${}^1S_0$ state. Parameters from the ${}^1S_0$ momentum-dependent fit.

V_T and V_D are the tensor and D-state potentials, respectively. We approximate the compact kernels of the integrals by matrices and $u(r)$ and $w(r)$ by column vectors u_r and w_r. Then Eq. (2.1) can be written

$$\sum_{r'} K_{rr'}{}^{\text{I}}u_{r'}=0 \qquad \text{for all } r \tag{2.2a}$$

and

$$w_r=\sum_{r'} K_{rr'}{}^{\text{II}}u_{r'}, \tag{2.2b}$$

where K^{I} and K^{II} are easily obtained by approximating Eq. (2.1) as a matrix equation. This can be seen as follows. Consider a system of p-coupled matrix equations:

$$Z=BZ, \qquad Z=\begin{pmatrix}Z^1\\ \vdots\\ Z^p\end{pmatrix}, \qquad B=\begin{pmatrix}B^{11} & \cdots & B^{1p}\\ \vdots & & \vdots\\ B^{p1} & \cdots & B^{pp}\end{pmatrix}, \tag{2.3}$$

where each Z^i is itself a vector of length n, gotten by approximating the wave function $Z^i(r)$ by a set of n discrete points, $Z_r{}^i$. Each entry B^{ij} is accordingly a finite $n\times n$ matrix which approximates the (ij) kernel of the coupled integral equations, as in Eq. (2.1) where $p=2$. The kernel consists of the product of the Green's-function matrix and the potential matrix. Then Eq. (2.3) can be further written

$$Z=\begin{pmatrix}\tilde{Z}\\ Z^p\end{pmatrix}, \qquad B=\begin{pmatrix}\tilde{B} & b\\ \bar{b} & B^{pp}\end{pmatrix}, \tag{2.4}$$

where $\tilde{Z}$ and b are column vectors (of n vectors) of length $p-1$ and $\bar{b}$ is a row vector (of n vectors) of length $p-1$, all gotten from Eq. (2.3); $\tilde{B}$ is a block matrix (of $n\times n$ matrices) of dimension $(p-1)\times(p-1)$.

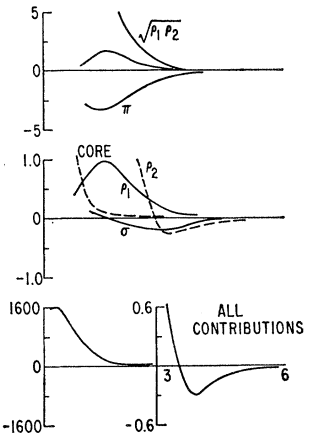

FIG. 4. Contribution of each meson to the static part of the interaction potential (BeV) versus $r(\text{BeV}/\hbar c)^{-1}$ in the ${}^3P_0$ state.

Then a solution for these equations is

$$[1-B^{pp}-\bar{b}(1-\tilde{B})^{-1}b]Z^p=0 \tag{2.5a}$$

and

$$\tilde{Z}=(1-\tilde{B})^{-1}bZ^p, \tag{2.5b}$$

where $(1-\tilde{B})^{-1}$ is a block matrix of dimension $(p-1)\times(p-1)$ such that

$$(1-\tilde{B})(1-\tilde{B})^{-1}=I, \tag{2.6}$$

where I is a block matrix of $(p-1)$ identity matrices along the diagonal. Sets of p-coupled inhomogeneous $n\times n$ matrix equations similar to Eqs. (2.5) can be solved for the p-coupled channels of the corresponding scattering and nuclear matter problems. The momentum-space equations are similarly treated.

The matrices K^{I} and K^{II} of Eq. (2.2) can now be read off from Eqs. (2.5) for the case being considered, when $p=2$. As shown in NF-Eq. (5.3), a reduced $(n-1)\times(n-1)$ matrix equation using the $n\times n$ entries of the matrix in square brackets of Eq. (2.5a) allows an easy numerical solution for the eigenvector Z^p,

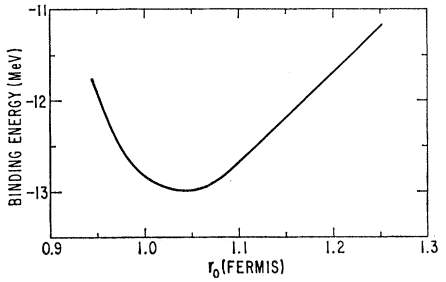

FIG. 5. Full binding energy versus r_0 calculated using the Reid potential.

from which the other eigenvectors included in $\tilde{Z}$ may be solved for using Eq. (2.5b). This can be done after the determinant of the matrix of Eq. (2.5a) has been adjusted to be small enough so that the eigenvector Z^p is finite [see Eq. (2.8)].

Equation (2.2a) is a mathematical statement of the eigenvalue condition necessary to solve the bound-state deuteron problem. The σ-coupling constant was varied to satisfy (2.2a) by demanding that

$$\det|K_{rr'}{}^{\mathrm{I}}|=0. \tag{2.7}$$

[The coupling constants of mesons considered here are defined in NF-Eqs. (2.1)–(2.5) in the phenomenological Lagrangians which couple these mesons to the nucleons.] Finite values of u_r numerically consistent, as explained below, with larger and finer meshes were found to be consistent with

$$\det|K^{\mathrm{I}}(g_\sigma{}^2 \text{ at minimum determinant})| \leq 10^{-8}\det|K^{\mathrm{I}}(g_\sigma{}^2 \text{ at "average" determinant})|. \tag{2.8}$$

The eigenvalue condition was satisfied for each value of another parameter, taken to be the π-coupling constant $g_\pi{}^2$, which was varied between 13.5 and 15.0. In this manner, it was possible to fit the quadrupole moment and the binding energy of the deuteron; the eigenfunctions and quadrupole moment were solved for as

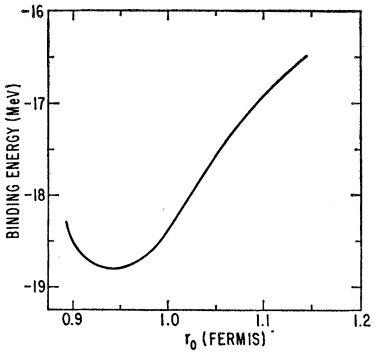

FIG. 6. Full binding energy versus r_0 calculated using the momentum-dependent potential for the S and ${}^3D_1$ states. A static potential (Reid) is used for the remaining states.

TABLE I. Parameters and properties of deuteron obtained in partial-wave fits. All masses are given in units of BeV/c^2, and g_{core}^2, the core strength, is given in units of BeV. Parameters that are fixed and common to all fits are $\mu_\pi=0.135$, $\mu_\eta=0.548$, $\mu_\rho=0.76$, $\mu_\omega=0.78$, $\mu_\varphi=1.02$. Four cutoff masses Λ_n in the Feynman-type regularization are used. These are computed from $\Lambda_n=[1+(n-1)\alpha_\Lambda]\Lambda_1$, where Λ_1 and α_Λ are parameters determined in each fit. Here $g_\varphi^2=g_\omega^2$, but one could take $g_\varphi^2=0$ (Ref. 12), and effectively double g_ω^2 since $\mu_\omega\approx\mu_\varphi$.

Potential	Waves fitted	g_π^2	g_σ^2	g_{P_1}	$g_{P_2}^2$	g_ω^2	g_η^2	g_{core}^2	μ_σ	m_c	m_s	m_m	Λ_1	α_Λ	f
Full momentum dependence	Deuteron+$^3S_1$ $+^3D_1+\epsilon$	15	2.238	1	30	2	13	11.66	0.42	1	0.811	0.5	0.876	1	66.1
	$^1S_0$	15	3.161	1	24.15	1	0	10	0.42	0.834	1.15	0.5	0.989	1	4.8
	$^1P+^3P_0+^3P_1+^3P_2$	13.5	4.2	2.202	28	2.318	0	2	0.52	1.047	1.1	2.6	1.889	1.406	315
	$^1D+^3D_1+^3D_2$	15	3.23	0.2	38	2.3	16	32.66	0.42	0.675	0.211	0.5	0.838	0.512	30.3
No momentum dependence (i.e., static part only)	Deuteron+$^3S_1$ $+^3D_1+\epsilon$	14	1.934	1.2	27.5	2	13	11.73	0.42	1	0.5	0.5	0.839	1	68.9
	$^1S_0$	15	3.179	1.176	25.79	1	0	10	0.42	0.834	0.7	0.5	0.982	1	15
	Computed properties of deuteron									Quadrupole moment (F^2)					
	Full momentum-dependent potential									0.281					
	Static potential									0.282					
	Experimental value									0.282					

described in NF-Eqs. (5.3)–(5.5). A minimum accuracy of 2% of the observed binding energy of the deuteron was demanded and our numerical accuracy was within this error. More accuracy just affected the third and fourths ignificant figures of the parameters; this did not appreciably affect the phase-shift calculation or the nuclear-matter calculation, which itself has larger errors due to the approximations of Brueckner and Masterson.[2] This is no surprise as the deuteron binding energy is obtained as a cancellation of potential and kinetic energy terms, each a full order of magnitude larger than the resultant binding energy, as explained in Sec. III D.

B. Problem (ii)—Scattering Phase Shifts

Data at incident laboratory energies of 25, 50, 95, 142, 210, and 310 MeV [1] were used to fit the calculated phase shifts δ. The function f minimized in the fit was

$$f=\sum[\delta_l(\text{expt})-\delta_i(\text{calc})]^2/[\text{expt error in }\delta_i]^2,$$
$$i=\text{expt points}. \quad (2.9)$$

Only for numerical expediency, the constraints of the full error matrix were not included in this fit. In Ref. 1, note the controversy over ϵ_1, the coupling parameter of the coupled $^3S_1$-$^3D_1$ states. The large experimental error in ϵ_1 allows the sort of flexibility in the C/T ratio at all energies, as discussed in Sec. III C.

C. Problem (iii)—Nuclear Matter

The same computational scheme, following Brueckner and Masterson,[2] as that reported in NF-Sec. IV was used here. Again, the Green's function was written as the sum of a simple function and an integral containing the exclusion-principle correction. This correction was found to be necessary only for the S state. The Green's function used was

$$G_l(r,r')=\alpha h_l(i\alpha r_>)j_l(i\alpha r_<)$$
$$+(\pi m)^{-1}\int_0^\infty dq''q''^2 j_l(q''r)j_l(q''r')$$
$$\times\{Q(p,q'')[E(q)-E^*(q'')]^{-1}-[E(q)-q''^2/(2m)]^{-1}\}. \quad (2.10)$$

Here $\alpha=[-2mE(q)]^{1/2}$, where $E(q)$ is the energy of a nucleon within the Fermi sea of nucleons in nuclear matter, commonly called a "hole." The quantity $E^*(q'')$ is the energy of a particle energy state outside of this Fermi sea (i.e., $q''>q_F$, q_F is the Fermi momentum bounding the Fermi sea). The exclusion-principle function $Q(p,q'')$ insures that the holes can scatter only to particle states outside the Fermi sea. The notation $r_>$ and $r_<$ and the functions j_l, h_l are as defined in Eq. (2.1). The energy denominators in the Green's functions for particles are shifted off the energy shell.[2]

At higher particle energies, corresponding to momenta above several Fermi momenta, higher-order density effects embodied in three-particle scatterings modify the particle-state energy spectrum. The results of Bethe and Day[6] are that these high-energy particle states should be labeled by simple kinetic energies, and that the states just above the Fermi sea should presumably be calculated self-consistently. We show in Sec. III A *2* that the contribution to the binding energy of the two-body part of the nuclear-matter calculation is insensitive to the energy spectrum just above the Fermi sea. The contribution of the three-body contribution is found to be less than 1 MeV.[6] We have also not included effects of three-particle potentials which can give about 2-MeV additional binding.[7]

D. Numerical Checks

The scattering $^1S_0$ state was solved using the Schrödinger differential equation as well as the Lippmann-Schwinger integral equation in coordinate space. This tested the matrix inversion method. The coupled $^3S_1$-$^3D_1$ state code with the tensor force set equal to zero and with the $^3S_1$-state potential set equal to the $^1S_0$-state potential gave the same wave functions for the $^1S_0$ state; this provided a limited check on the coupled-equations code. In addition, the Reid soft-core potential[8] was used to calculate the properties of the deuteron, the phase shifts, and the binding energy of nuclear matter. Complete agreement was obtained between these calculations and Reid's published results. The mesh used in all calculations with the meson-exchange potential was determined by requiring the associated Compton wavelength of the dominant meson, and that of the associated Green's function of problems (i), (ii), and (iii) above, be spanned by several points for use with Simpson's rule. Simpson's rule was used because of the simplicity in treating the step-function part of the potential arising with momentum-dependent potentials (see NF-Sec. V B). Each calculation was checked as to the best minimum number of mesh points (31), and as to the smallest end point [35 BeV/$(\hbar c)$] which was necessary for the deuteron calculation.

TABLE II. Nuclear-matter binding-energy data for the Reid potential tabulated as a function of r_0, the average nucleon spacing. In this and the following two tables, when partial-wave contributions are given, these are contributions to the single-particle potential energy; the average kinetic energy $0.6q_F^2/(2m)$ is not included. The Pauli exclusion principle is included in the S states. The partial-wave contributions are computed using the self-consistent (hole) spectrum from the full binding calculation.

Contributing partial waves	r_0 (F)	Energy (MeV)
Full binding energy	0.95	−11.87
	1.0	−12.82
	1.12	−12.59
	1.25	−11.18
Full binding energy with particle spectrum, $E^*(q)=q^2/(2m)$	0.95	−12.42
	1.0	−12.84
	1.12	−12.34
$^3S_1+^3D_1$	0.95	−14.95
	1.00	−15.24
	1.12	−14.79
	1.25	−13.44
$^3S_1$	0.95	−17.59
	1.00	−17.43
	1.12	−16.22
^1S	1.0	−18.49

TABLE III. Nuclear-matter binding-energy data computed with momentum-dependent potential for the S and $^3D_1$ states. A static potential (Reid) is used for the remaining states. See Table II.

Contributing partial waves	r_0 (F)	Energy (MeV)
Full binding energy	0.90	−18.50
	0.94	−18.80
	1.00	−18.33
	1.12	−16.72
Full binding energy with particle spectrum, $E^*(q)=q^2/(2m)$	0.87	−18.26
	0.90	−18.73
	1.0	−18.18
	1.12	−16.09
$^3S_1+^3D_1$	0.94	−19.45
$^3S_1$	0.94	−19.27
^1S	0.94	−19.75

III. POTENTIALS

A. Momentum-Dependent and Reid Potentials

The momentum-dependent potentials used in this work did differ slightly from the potentials used in NF. The meson contributions were the same as in NF and the momentum expansion and dependence were treated exactly as outlined in NF-Sec. II, but the small-r region within $r < \hbar(mc)^{-1}$ was treated differently: Examination of NF shows that delicate adjustments of the very sensitive momentum-dependent relativistic region [here defined in coordinate space as belonging to $r<\hbar(mc)^{-1}$] was instrumental in getting a simultaneous fit to the scattering data in S, P, and D waves with parameters common to all these partial waves.

[6] B. D. Day, Rev. Mod. Phys. **39**, 719 (1967); R. Rajaramann and H. A. Bethe, *ibid.* **39**, 745 (1967); B. H. Brandow *ibid.* **39**, 771 (1967).

[7] G. E. Brown and A. M. Green, in Three-Body Forces in Nuclear Matter (to be published).

[8] R. V. Reid, Ann. Phys. (N.Y.) **50**, 411 (1968).

TABLE IV. Nuclear-matter binding-energy data computed with the static part of the meson-exchange potential in the S and $^3D_1$ states. A static potential (Reid) is used for the remaining states. See Table II.

Contributing partial wave	r_0 (F)	Energy (MeV)
Full binding energy	0.94	−17.19
	1.00	−17.50
	1.12	−16.3
Full binding energy with particle spectrum, $E^*(q)=q^2/(2m)$	0.94	−17.38
	1.00	−17.40
	1.12	−15.99
$^3S_1+^3D_1$	1.0	−15.92
$^3S_1$	1.0	−18.32
^1S	1.0	−20.36

Within this relativistic region, by virtue of solving Schrödinger's equation, we have already professed complete ignorance of the physics relating to processes where $r<\hbar(mc)^{-1}$ and/or where the magnitude of the potential energy is greater than that of the kinetic energy. If such calculations as we perform here are to make sense, they must be independent of the structure of the cutoffs and physics of this region. Therefore, it was of interest to try a different functional form for the potential in the relativistic region. More precisely, if these calculations can be sensibly formulated by nonrelativistic Schrödinger's equations, then the relativistic region should at least be shape-independent, or at most dependent on two parameters corresponding to the depth and range of the potential in this region. Therefore, a Gaussian core was added of the form

$$g_{\text{core}}^2 \exp[-(m_c r)^2]. \tag{3.1}$$

The rest of the potential was cut off by other Gaussians for the static and momentum-dependent functions:

$$\mathfrak{v}(\text{static})\rightarrow\{1-\exp[-(m_s r)^2]\}\mathfrak{v}(\text{static}) \tag{3.2}$$

and

$$\mathfrak{w}(\text{momentum})\rightarrow\{1-\exp[-(m_m r)^2]\}\mathfrak{w}\,(\text{momentum}). \tag{3.3}$$

The functions $\mathfrak{v}$ and $\mathfrak{w}$ contribute to the total potential $V(\text{total})$, in the form

$$V(\text{total})=(\mathfrak{v}-\tfrac{1}{2}d^2\mathfrak{w}/dr^2)-(d\mathfrak{w}/dr)(d/dr)-\mathfrak{w}(d^2/dr^2). \tag{3.4}$$

1. Scattering and Deuteron Fit

We left some flexibility in the ranges of the cutoffs by parametrizing m_c, m_s, and m_m in Eqs. (3.1)–(3.3) in order to see how sensitive the potential would be to these cutoffs. The high-mass Feynman-type regularizations used to cut off the potentials in NF-Sec. IV were retained to prevent still persistent deep sharp dips in the potentials due to the short range of the Gaussian cutoffs. Table I gives the final parameters necessary to obtain the indicated fits. Notice we calculated a 4.6% D state for the deuteron. The S, P, and D waves were separately fitted to give the same value of the function f, defined in Eq. (2.9), as the Reid potential.[8] Figures 1–4 give plots of the contributions of individual mesons to those parts of the $^3S_1$, tensor, $^2S_0$, and $^3P_0$ potentials which are expressed as $(\mathfrak{v}-\frac{1}{2}d^2\mathfrak{w}/dr^2)$ in Eq. (3.4).

2. Nuclear Matter

The $^1S_0$, P, and D waves for this potential gave the same contributions, within an MeV, to the nuclear-matter binding energy as with the Reid potential. We therefore confine most of the discussion to the coupled $^3S_1$-$^3D_1$ state in order to further discuss differences between this and previous nucleon-nucleon potentials. Table II gives the results of our calculations using the Reid potential, broken down to the $^3S_1$-$^3D_1$, $^3S_1$ alone (with the tensor force set equal to zero), and to the $^1S_0$ states. A static $^3D_3$ potential, appropriately fitted to the scattering data, was supplemented when using the Reid potential. Figure 5 gives the saturation curve (binding energy per particle versus r_0, the equilibrium distance) for the self-consistent (particle states and holes) nuclear-matter calculation, as outlined in NF-Sec. III, using the Reid potential.

Table III gives the breakdown by partial wave for the contributions to the binding energy for the momentum-dependent potential, and Fig. 6 gives the saturation curve using the momentum-dependent potential for the singlet and triplet S states; the Reid potential was used for the P and D states. Figure 7 gives the saturation curve using a self-consistent energy spectrum for the holes only in the exclusion-principle integral in Eq. (2.10); a free kinetic-energy spectrum

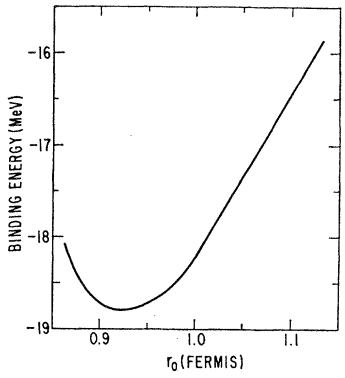

FIG. 7. Full binding energy versus r_0 calculated using the momentum-dependent potential for the S and $^3D_1$ states; a static potential (Reid) is used for the remaining states. The particle spectrum $E^*(q)$ is set equal to $q^2/2m$.

was used for the intermediate particle states. It is to be noted that there is little difference in the value and position of the binding energy at saturation between Figs. 6 and 7, apparently contrary to Masterson,[9] who states that consistency must be included for the particle states if saturation is to be achieved. The point is that *after* a self-consistent hole spectrum giving saturation is achieved, *then* their results are insensitive to the particle-state energy spectrum.

3. Comparison with NF

Although a large binding energy per particle in nuclear matter was achieved in this work (−18.8 MeV) as in NF (−14.6 MeV), r_0 dropped from 1.15 F in NF to 0.95 F here. Also, decreasing the sensitivity of the cutoffs in the relativistic region and demanding a deuteron fit did shift the values of the other meson-coupling parameters, especially that of the σ meson (see NF-Sec. II B). More will be said about this below.

B. Static Potential

1. Scattering and Deuteron Fit

In Sec. III A, we modified the momentum-dependent potential of NF to allow the nonrelativistic region to exhibit shape independence, i.e., to depend just on the range and depth of the potential in this region. We tested this approach even further by investigating the *minimal* important contributions of the momentum dependence. We examined the momentum-dependent potential and attempted to find a static function which would resemble the shape of the momentum-dependent potential Fig. 8. We found that only small adjustments of parameters were necessary to fit the deuteron and phase-shift data even if we kept the static part of Eq. (3.4), obtained by dropping the last two terms. The reason for this is discussed in Sec. III B *3*. The bottom half of Table I gives the resulting parameters using the static potential. Again note that we also obtain a small percent D state for the deuteron, at 5.5%.

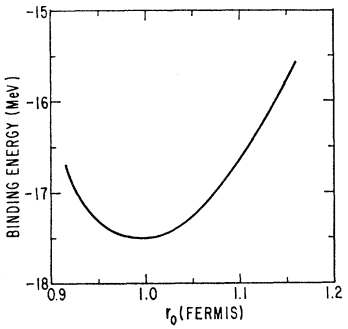

FIG. 8. Full binding energy versus r_0 calculated using the static part of the meson-exchange potential in the S and $^3D_1$ states. A static potential (Reid) is used for the remaining states.

[9] K. S. Masterson, Jr., Ph.D. thesis, University of California at San Diego, 1963 (unpublished).

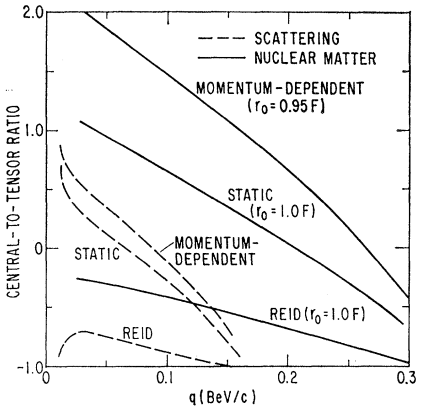

FIG. 9. Central-to-tensor ratio C/T versus q. Curves are computed from the three types of potentials, momentum-dependent and static meson-exchange potential, and the Reid potential. The nuclear-matter ratios are evaluated at the average particle separation r_0 nearest the saturation point for the corresponding potential.

2. Nuclear Matter

We obtain the same binding energy per particle using the static potential as with the momentum-dependent potential. This shows that the momentum dependence may also be treated in various phenomenological fractional forms, as its major contribution is in the term $-\frac{1}{2}d^2w/dr^2$ of Eq. (3.4). In Sec. III C, we discuss why we still get about 5 MeV more binding energy than other investigators using other potentials have previously obtained.

3. Sensitivity of Momentum Dependence

There exists some change in the parameters obtained with the static potential versus those obtained with the momentum-dependent potential. Also, the shape of the saturation curve (compressibility) of the nuclear-matter calculation is obviously different. It is easy to understand why the saturation properties show the largest sensitivity to the momentum dependence: The operator d/dr' in the potential of the deuteron, Eq. (2.1), enters similarly in the nuclear-matter problem. The principal difference in the nuclear-matter equation [see NF-Eq. (4.6)] is that the first matrix factor of Eq. (2.1) now contains the Green's function as described by Eq. (2.10). Integration by parts allows us to write Eq. (2.1) so that the (d/dr') operators, as in Eq. (3.4), all operate on the Green's functions. Then it is straightforward to see that

$$d/dr' \rightarrow \alpha[dG_l(r,r')/dr']/G_l(r,r'),$$
$$d^2/dr'^2 - l(l+1)/r^2 \rightarrow \alpha^2, \qquad (3.5)$$

where $\alpha=[2mE(q)]^{1/2}$, as in Eq. (2.6). The quantity $E(q)$ varies with the value of the Fermi momentum q_F and gives rise to the density dependence which makes the saturation properties of nuclear matter more sensitive to the momentum-dependent potentials, as com-

pared to the static potentials. The similarities between the two potentials arise from the fact that terms introduced by expressions similar to Eq. (3.5) involve α [in Eq. (2.6)], γ [in Eq. (2.1)], or q [Eq. (1.5)], which are all $<m$ in these calculations. In Sec. IV, we also discuss the importance of the two-pion-exchange region to the nucleon-nucleon interaction. We feel that conclusions about the calculations presented here comparing our static and momentum-dependent potentials are not complete until the physics as discussed in Sec. IV is included in these types of calculations and analyses.

C. Central-to-Tensor Ratio

The 5-MeV extra binding in the coupled $^3S_1$-$^3D_1$ partial waves from these momentum-dependent and static potentials derived from meson-exchange amplitudes, as compared to the Reid and previous phenomenological potentials, can best be understood by comparing the diagonal to off-diagonal matrix elements. That the ratio of these matrix elements has not been accurately pinned down by the experimental data has been noted for some time, and this effect on the nuclear-matter binding energy was noticed by Brueckner and Masterson.[2] It appears that recent data at 24- and 25-MeV incident laboratory scattering energies do more accurately contain this parameter. These newer data were not known at the time these calculations were performed. Of course, the nuclear-matter binding energy is also a number derived from experiments and this number should also be fitted by a nucleon-nucleon interaction.

The coupled equations in the α channel for the scattering problem may be formally written, similar to Eq. (2.1) for the deuteron,

$$(qr)^{-1}\begin{pmatrix} u \\ w \end{pmatrix} = \begin{pmatrix} j_0 \\ 0 \end{pmatrix} + mq \int r'^2\, dr' \begin{pmatrix} j_0 n_0 & 0 \\ 0 & j_2 n_2 \end{pmatrix} \times \begin{pmatrix} V_S & V_T \\ V_T & V_D \end{pmatrix} \begin{pmatrix} u \\ w \end{pmatrix} (qr')^{-1}, \quad (3.6)$$

where j_l and n_l are spherical Bessel and Neumann functions of order l, and the indices and arguments are now obvious enough to be suppressed for clarity. The u-state phase shift is the sum of two matrix elements which we denote by C and T:

$$(j_0, V_S u) + (j_0, V_T w) = C + T, \quad (3.7)$$

respectively. The quantities C and T are, of course, functions of energy, labeled by q^2/m as in Eq. (1.2) for the scattering problem, or by $\gamma^2(-q^2=m\epsilon)/m$ as in Eq. (2.1) for the deuteron problem, or by $\alpha^2(q^2)/m$ as in Eq. (2.10) for the nuclear-matter problem. Figure 9 gives the ratio of C/T for the Reid, the momentum-dependent, and the static potentials for both the scattering and the nuclear-matter problems. Note that for each potential, the slope of C/T is about the same for the scattering and nuclear-matter problems. This is so because the inhomogeneous terms, Bessel functions, of the integral equations and the Bessel functions that enter into the calculation of the nuclear-matter matrix elements, as written in NF-Eq. (4.7), have the same momentum variable q^2 as in the scattering case. On the other hand, the conjugate variable of the nuclear-matter Green's function in Eq. (2.10), α^2, is relatively constant over this same range and therefore does not affect the *ratio* C/T as much as the Bessel functions. This is true for various values of r_0 for each potential, as can be seen in Fig. 10 on which is plotted the C/T ratio for various values of r_0 for the momentum-dependent potential.

At low energies, for the potentials we use here, the plots in Fig. 9 are a result of

$$C/T = (+ \text{ large})/(+ \text{ small}). \quad (3.8)$$

However, for previous potentials, as the Reid potential, the C/T ratio at low energies is a result of

$$C/T = (+ \text{ small})/(- \text{ large}). \quad (3.9)$$

Note that the *sum* of $C+T$ in Eq. (3.7) enters into the calculation of the nuclear-bar $^3S_1$ eigenphase shift, and the phase shift has been fitted equally well for both C/T ratios of Eqs. (3.8) and (3.9). This can be further understood by comparing the actual potentials used by Reid to our static potential which gives essentially the same results as our momentum-dependent one. The Reid central and tensor potentials are given in Figs. 11(a) and 11(b). The Reid potential shows a smaller

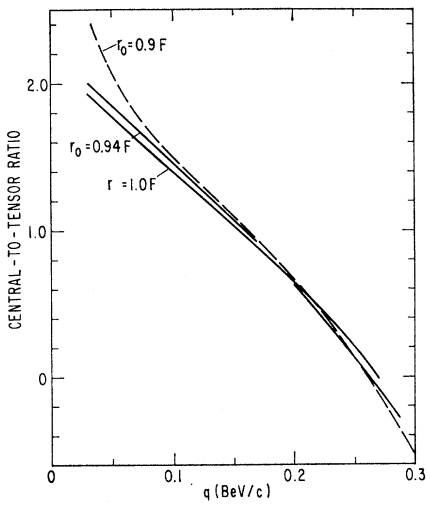

FIG. 10. Nuclear-matter central-to-tensor ratio C/T versus q computed with the momentum-dependent potential at various r_0.

central force than Fig. 1 shows for the static potential; it also shows a larger tensor force than Fig. 2 shows for the static potential.

A possible reason only one type of functional form of central and tensor potential has persisted for over 25 yr [10] is that ever since the use of one-pion-exchange potentials for the large-r part of the nucleon-nucleon interaction, the tensor force has been cut off at about 0.4–0.5 F, allowing it to diverge towards the origin as $\sim r^{-3}$ until being cut off. It would be practically impossible for a local-search computer program to go from one region of C/T as calculated previously, to another as we calculate, without going through a region of enormous values of the function f in Eq. (2.9). Better data of ϵ_1 at 25 MeV [1] will put further restrictions on the C/T ratios which can be allowed for a nucleon-nucleon potential.

D. Overview of Potential and Connection of Deuteron and Nucleon-Matter Binding Energies

Examination of the associated Compton wavelengths of the Green's functions used in nuclear matter [α in Eq. (2.10)], the scattering problem [q in Eq. (1.2)], and for the deuteron [γ of Eq. (2.1)] reveals the regions of sensitivity of these various physics problems. This is illustrated in Fig. 12. It is clear that a nucleon-nucleon potential is defined throughout the nonrelativistic region only if it is capable of being in agreement with the experimental data of these three physics problems. The utility of this point of view is that we are able to interpret simply the observation that the binding energy of nuclear matter is very sensitive to the quadrupole moment of the deuteron.

The quadrupole moment of the deuteron is sensitive

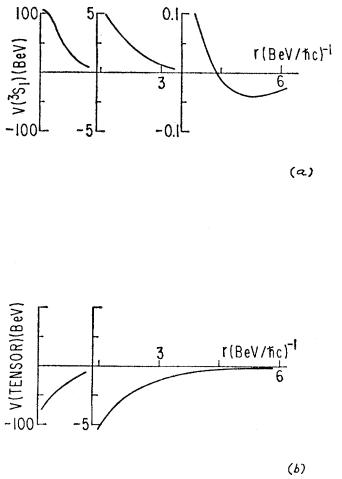

FIG. 11. (a) Plot of the $^3S_1$ Reid potential versus r. (b) Plot of the Reid tensor potential versus r.

[10] H. A. Bethe, Phys. Rev. **57**, 260 (1940).

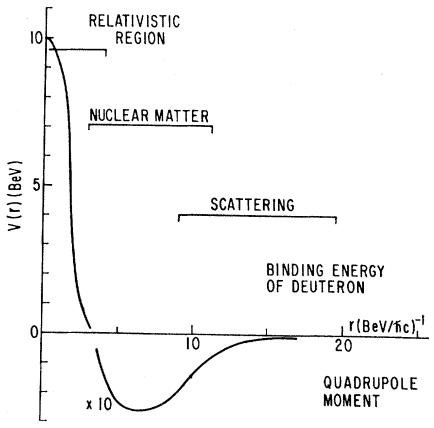

FIG. 12. Display of the general regions of sensitivity of nuclear properties to the nuclear potential in coordinate space. The qualitative shape of the static part of the S-state potential is shown. The coordinate r is given in units of $(\mathrm{BeV}/\hbar c)^{-1}$, where the conversion factor from fermis to $(\mathrm{BeV}/\hbar c)^{-1}$ is 1 F$=5.0686$ $(\mathrm{BeV}/\hbar c)^{-1}$.

to the bulk cancellation of the repulsive and attractive parts of the potential as this affects the normalization of the deuteron wave functions, which effects the asymptotic wave functions past the range of the potential, which gives the major contribution to the quadrupole moment. However, in also fitting the binding energy of the deuteron, this net potential of about -20 MeV is determined and further added to the similarly large kinetic energy to give the net value of -2.22452 MeV.

The cancellation of the repulsive and attractive parts of the potential is most directly influenced in the region where the potential changes sign. This is precisely the region most sensitive to the nuclear-matter calculation. Further, the nuclear-matter calculation is also similar to the deuteron-binding-energy calculation in that the nuclear-matter binding energy is itself a number determined by a delicate cancellation of two large numbers, the sum of the average kinetic and potential energies.

IV. δ MESON

If the physics of the one-meson-exchange amplitudes provided a complete description of the nonrelativistic nucleon-nucleon interaction, then one would expect that all three of the above physics problems would be described by a potential containing the masses and coupling constants of the meson-nucleon system, *independent of partial wave*, and within reasonable experimental errors. Table I definitely shows this is not true.

We tentatively affix "blame" for this condition on the σ meson which we feel does not adequately describe the physics of the two-pion-exchange region of this interaction. Indeed, even with the increased sensitivity achieved with the low mass of the σ meson, one cannot

achieve good fits with parameters independent of partial wave. We propose that this causes the necessary subsequent adjustment of the other meson couplings and of the core region to accomplish the sensitive cancellations necessary for good agreement with the experimental data.

In fact, if the inclusion of the "correct" physics would replace the σ meson, then, as shown in Sec. II A, the deuteron problem would be sensitive enough to permit an accurate determination of the π-nucleon coupling constant.

These three problems above can also be used to assess the correctness of the various possible contributions to this intermediate region of the nucleon-nucleon interaction. Contributions under investigation are the two-pion-exchange amplitude,[11] N^* intermediate states in two-pion-exchange amplitudes,[12] Reggeization of the ρ meson,[13] and low-energy π-nucleon scattering theory.[14] Effects of other higher-mass baryons and other mesons than considered here appear to give negligible contributions not only in the σ meson region, but throughout the nonrelativistic region.[15]

V. CONCLUSION

We have given strong arguments to show that a nonrelativistic nucleon-nucleon potential must give agreement with the deuteron binding energy and quadrupole moment, the scattering data between 25- and 310-MeV incident laboratory energy, and the binding energy and saturation property of nuclear matter. We have calculated both momentum-dependent and static phenomenological potentials, derived from one-meson-exchange amplitudes, which accomplish these tasks reasonably well. These potentials do this by virtue of having different central and tensor components than previous potentials.

We also give plausible arguments that we have been forced to phenomenological potentials defined separately in each partial wave because the σ meson at $\sim$400 MeV is not a physical meson and the actual physics of the two-pion region must be calculated and analyzed similar to the analysis of the potentials presented here. We then claim the success of this program can be tested by achieving a two-parameter nucleon-nucleon potential, satisfying the above criteria, in which only the range and depth of the relativistic region is parametrized.

ACKNOWLEDGMENTS

We are grateful to Keith A. Brueckner for many stimulating conversations and suggestions. It is also a pleasure to acknowledge the services of the 3600 CDC computer staff at UCSD, whose courtesy and efficiency made these calculations possible. One of us, Lester Ingber, would like to further acknowledge the hospitality of the Physics Department at UC, Berkeley (particularly Kenneth Watson), and the Physics Department at UC, Los Angeles (particularly Steven Moszkowski), where this author was an NSF postdoctoral fellow. During these two years, the IPAPS staff and faculty, guided by Keith A. Brueckner and Bernd T. Matthias, made this joint work possible.

---

[11] M. H. Partovi and E. L. Loman, Phys. Rev. Letters **22**, 438 (1969).

[12] H. Sugawara and F. von Hippel, Phys. Rev. **145**, 1331 (1966). This paper also contains a nice discussion of SU_3 as applied to g_η^2 and g_φ^2 (both should be $\sim$0), and of the electric and magnetic couplings of the ρ meson.

[13] A. Jackson (private communication). This is one way of putting physics into the core region.

[14] R. Dashen andM. Weinstein, in Soft Pions, Chiral Symmetry, and Phenomenological Lagrangians (to be published).

[15] W. Wortman, Ph.D. thesis, Texas A & M University, 1968 (unpublished).